WORLD NEWS | Special Article
Arch. Esp. de Urol., 53, 4 (291-303), 2000

Nanobacteria. An experimental model of neolithogenesis.

ENRIQUE GARCÍA CUERPO*, EINO OLAVI KAJANDER[2], NEVA ÇIFTÇIOGLU[2], FRANCISCO LOVACO CASTELLANO[1], CARLOS CORREA[6], JAVIER GONZÁLEZ[3], FRANCISCO MAMPASO[4], FERNANDO LIANO[5], ENRIQUE GARCÍA DE GABIOLA[7] AND ÁNGEL ESCUDERO BARRILERO[7].

[1]Department of Urology (Prof. A. Escudero). Hospital Ramón y Cajal. Universidad de Alcolá. Madrid, Spain
[2]Department of Biochemistry and Biotechnology (Prof. E. O. Kajander). University of Koupio, Finland
[3]Department of Microbiology (Prof. F. Baquero). Hospital Universitario Ramón y Cajal. Madrid, Spain
[4]Department of Pathological Anatomy (Prof. F. Mampaso). Hospital Universitario Ramón y Cajal. Madrid, Spain
[5]Department of Nephrology (Prof. J. Ortuño). Hospital Universitario Ramón y Cajal. Madrid, Spain
[6]Experimental Surgery Unit. Hospital Universitario Ramón y Cajal. Madrid, Spain
[7]University Teaching Support Department (Prof. C. Vizcarro). I.C.C. of Education. UAM
**Experimental Project Coordinator*

To Luis Cifuentes Delatte and José María Gil-Vernet, in recognition of their support in the research and surgical treatment of urinary lithiasis.

[Italian verse translated below from the Spanish.]

Like that stream, which issues from the Bulicame*
whose waters the prostitutes share,
this stream flowed down across the sand.
The bed was of stone, as were both banks
and the borders running alongside
So that I perceived our way across lay there.

(*Divine Comedy*. The Inferno, Verse XIV. 79-84)

*Cave 2 km from Viterbo where Dante placed the gates of hell.

Correspondence
E. García Cuerpo
C/. Clara del Rey, 33
28002 Madrid, España
Work received May 5, 2000.

[Summaries in Spanish and English]

INTRODUCTION

The complex biomineralization processes that occur in nature have occupied researchers in fields as diverse as geology, bacteriology and urology. Our interest here is centered on the processes that give rise to lithiasic pathology, a disease that affects 4.16% of our population (1) and causes high morbidity.

The chapter begins with Cifuentes, C*alcium phosphates of the apatite series* (2), a series which begins as *hydroxyapatite*, the most alkaline phosphate, which has a molar ratio of Ca/P = 1.66, giving it greater complexity. It almost always contains CO3-- in its cryptocrystalline network, also called *carbonate apatite,* and it is not a compound that has a closed chemical formula (Fig. 1).

Forms of apatite:

1. Those that replace OH groups (A-type carbonate apatite).
2. Carbonatoapatite B, by replacing groups (PO4).
3. Carbonate apatite AB. Formed by replacing both groups. This is the predominant form in renal calculi. Dr. Magna Santos corroborates these findings in her doctoral thesis on apatites (3).

According to Cifuentes, in the lithiasic nucleation mechanisms, *it does not appear impossible for other spherulites to be able to have a center structure on which crystals grow in a radial arrangement, but verification of this is a subject for future research*.

With the *Free Particle Theory* ruled out in practice by multiple experiments such as those of Finlayson or the researchers at the Universidad de Jena, we accept the *Fixed Particle Theory* observed by Carr in the lymph nodes and in the renal papilla. Randall (4) calls attention to two fundamental characteristics in this process:

1 – The presence of calcification or initial lithiasic core in a large number of cases.

Of the 265 calculi that he examined, 40% had a whitish, finely granulated and irregular zone at the base of the calculus that was almost always concave corresponding to its adaptation to the end of the renal papilla. This is the Type I plaque that takes the von Kossa staining method by calcium salts that are observed in the interstitial tissue of the papilla. There are no intratubular deposits. They are currently discovered incidentally by nephroscope during the course of the percutaneous treatment for renal lithiasis. Analysis shows a phosphate and calcium carbonate composition, while the calculus could be primarily calcium monohydrate oxalate, the most common case. In Randall's Type II lesion, the calcification is intratubular, usually affecting multiple papillas and shows yellow lines that converge toward the end where mineral deposits are visibly pervasive in the cribriform membrane.

2 – The extremely slow time period between the formation of this core and the appearance of clinical symptoms.

In 1972, there were two contributions to this slow nucleation mechanism. From a geology viewpoint, Mitterer (5) analyzes special situations of lithogenesis in turbulent fluids in formations called *oolites*. In the Second Urology Course organized by Solé-Blacells, *Avances in Díagnostico y Terapéutica Urológica* (Advances in Urological Diagnosis and Treatment), Cifuentes describes similar phenomena of *oolitization* in caliceal diverticula. Borovia and Leiva found them in pyelogenic cysts (cited by Alonso and Somacarrera, 6). They are called *milk-of-calcium renal stones,* or *kalkmilch* in German, a special type of renal lithiasis.

Struvite lithogenesis, principally coralliform lithiasis, produced by *ureolitic germs* (7, 8, 9, 10, 11, 12) and *incrusted cystitis* due to *Corynebacterium* (13) are major contributions from urology and clinical microbiology to knowledge of biomineralization phenomena.

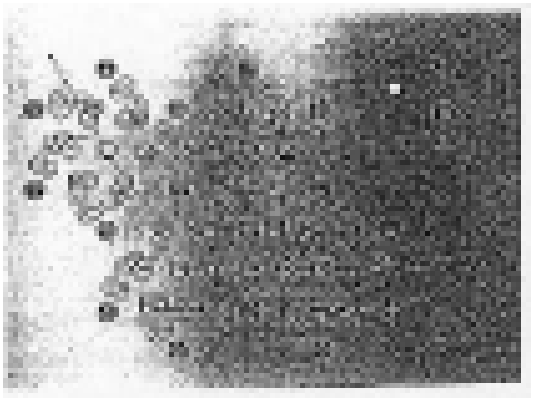

Fig. 1: Spatial arrangement of atoms in hydroxylapatite according to Kay. The unit cell is marked with lines between OH groups (Nature, 204: 1050, 1964).

Bacteriologists have studied microbial participation in geology:

1 – Krumbein (14) and through seaweed La Rock and Erlich (15).

2 – Robert L. Folk (16) sees cases similar to the previous ones in travertine marble, *lapis tiburtinus* of the Romans, and in the hot sulfur springs in *Bulicame** and *Bagnaccio* near Viterbo. Chafetz found them in Idaho and Yellowstone (USA) and in interior areas of Morocco (17).

3 – Allan Pentecost and the same Folk (18) describe different types of bacteria that occur in travertine:

3a – Photosynthetic bacteria.

3b – Chloroflexus in relation to the metabolism of sulfur.

3c – Some cyanobacteria with the capacity to precipitate aragonite.

4 – In the carbonate deposits near Viterbo, the *cannibalized* aragonite crystals are transformed into calcite. The surface of these crystals is surrounded by *mucus, glycocalix or biofilms*, a mucoprotein material with a high affinity for calcium salts, and to a lesser extent Mg, where the product [Ca++] x [CO3--], by greatly exceeding saturation, gives rise to the nucleation of carbonatoapatite around the bacteria.

5 – In the midst of these findings, the chapter has only just begun when new apparently contradictory data appear. In Viterbo, Folk found some spherical structures between 0.1 and 0.5 mm in size. For other authors, they are artifacts due to the reaction of the samples studied with acetic acid. For him, they are *nanobacteria* that are completely invisible to the ordinary microscope given their size. Observed under the *Scanning electron microscope* (SEM-EDS), they will be *artifacts* for some, *bacterial spores or residual phases* for other researchers, while to Kajander the ultramicrobateria or *nanobacteria* have the capacity to form very abundant dense colonies in the center of calcium crystals, which involves them in the nucleation process. They are not artifacts or biological remains. Çiftçioglu, Peltarri and Kajander identified them in mammalian blood (19) and in 5% of the population of the city of Kuopio, Finland (20). Research conducted over the last fifteen years by Eino Olavi Kajander, Neva Çiftçioglu and their team has isolated, identified and cultured *nanobacteria* in special environments, although neither Mark Plausic nor David Y. Chan (21) were able in their pilot study to verify the 16 sRNA sequence or the antigenic presence of *nanobacteria* in kidney and serum samples. From this basis, we intended to show by experimentation, the role that *nanobacteria* can play in extracellular calcification mechanisms of specific relevance in Urolithiasis (22).

EQUIPMENT AND METHODS

Four eight-week-old Brown Norway rats weighing 150 g were selected. Percutaneous renal puncture (PRP) of the left kidney was performed with a fine needle under inhalation anesthesia (induction with 4% isoflurane maintained at 2% with 1 liter/minute of oxygen). This side was selected to avoid puncturing the liver when accessing the renal parenchyma, without perforating the excretory path. 150 µl of a *Phase 1 Seralab 901045 nanobacteria* suspension was injected (Fig. 2), the concentration of which has not been possible to determine to date. The culture in DMEM medium was centrifuged at 40,000 x g for 60'. It was resuspended in PSB and centrifuged again at 40,000 x g for 90'. Finally, it was washed in saline solution. A control rat was injected with the same volume of saline serum only, without the bacterial load (Fig. 3), and the remaining [rats were injected] with successive loads double the previous, as shown in Table 1.

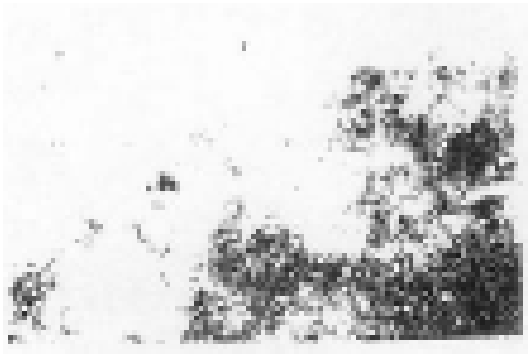

Fig. 2. Sample of nanobacteria culture to be inoculated in rats. Giemsa x 100.

Fig. 3. Area of percutaneous renal puncture (PRP) in the control rat, No. 4.

To Baquero, *nanobacteria are apparently a new group of microorganisms, with which he has little experience, but which, according to published information and that directly communicated by their discoverers, are probably ubiquitous, found in both healthy humans and animals as well as cultured cellular environments, and could assimilate a behavior similar to that of saprophyte mycoplasma. We do not know of any other relationship to the pathology other than one that is very indirect in relation to its capacity to build minerals, and therefore influence the development of extra cellular calcification and lithiasis.*

On the seventh and fourteenth days, blood samples were drawn to determine the creatinine, calcium and uric acid levels by autoanalyzer. On these days in which urine was collected 24 hours, the rats remained in metabolic chambers consuming 7 g of the food A03 (PANLAB, S. L. Barcelona, Spain) with the following composition ingested in 24 h. (Fig. 4):

Protein: 23.56%. Fat: 3.96%. Cellulose: 3.46%. Ash: 5.38%. Sodium: 21 mg. Potassium: 55.2 mg. Calcium: 55.2 mg. Phosphorous: 45.5 mg. Magnesium: 12 mg. Iron: 1.96 mg. Vitamin A: 117.6 IU. Vitamin D3: 21 IU. Also Vitamin E.

It was proven that the liquid balances were in equilibrium. In the 24 h. and 2 h. urine collection, for the pH, the degree of turbidity and volume were observed. The following parameters were determined by autoanalyzer: proteinuria, with an additional electrophoretic spectrum (EPS), glucose, creatinine, calcium, phosphorous and uric acid. The oxalic acid in the urine was determined by enzyme reaction. The glomeruler filtrate was estimated by determining the creatinine clearance.

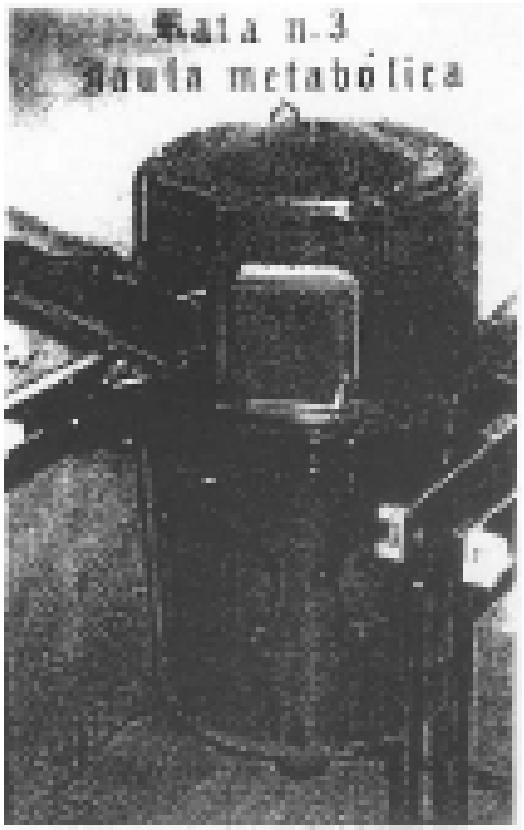

[Photo: Rat No. 3, Metabolic Chamber]

Fig. 4: Detail of the metabolic chamber of Rat No. 3

TABLE I				
EXPERIMENTAL LITHOGENESIS IN RATS				
Translumbar Percutaneous Renal Puncture Inoculation: nanobacteria culture washed in saline solution				
Rats	Inoculation	Dilution	Analysis	Radiology
No. 1	150 µl	1/10 in saline s.	Days: basal, 7, 14 and 21	Weeks 2 and 3
No. 2	150 µl	1/5 in saline s.	Days: basal, 7, 14 and 21	Weeks 2 and 3
No. 3	150 µl	½ in saline s.	Days: basal, 7, 14 and 21	Weeks 2 and 3
No. 4	150 µl	saline serum	Days: basal, 7, 14 and 21	Weeks 2 and 3

TABLE II								
EXPERIMENTAL LITHOGENESIS								
Basal Study of Renal Function								
Rats	Ingestion	Diuresis	Vol./mi	CrO	CrO	CrS	CCr	Weight
	(expressed in ml)			(mg/24h)	(expressed in mg/dl)		(µl/min. x 100 g)	(g)
No. 1	9.5	11	0.0076	9.7	88	0.60	779	143
No. 2	9	10.5	0.0073	11	105	0.55	995	140
No. 3	9.5	10	0.0069	9.8	98	0.53	911	140
No. 4	10	10.5	0.0073	9.3	89	0.50	896	145

TABLE III							
EXPERIMENTAL LITHOGENESIS							
Normal Phosphorus and Calcium Values							
Rats	CaS	CaO	CaO	PO	PO	pH	O Vol.
	(mg/dl)	(mg/24h)	(mg/dl)	(mg/24h)	(mg/dl)		(ml)
No. 1	10.2	1.12	12.4	15.5	159	8	9
No. 2	10	1.16	11.6	15.8	158	8.1	10
No. 3	9.4	1.10	12.3	14.9	148	8	9
No. 4	10	1.08	10.8	16	160	7.9	9.8

TABLE IV					
EXPERIMENTAL LITHOGENESIS					
Basal Values of Uric Acid					
Rats	O. uric acid /24 h	O. uric acid mg/dl	Cr O mg/24h	Cr O mg/dt	Uric acid/Cr
No. 1	1.15	12.7	10	111	0.11
No. 2	1.20	12	9.8	98	0.12
No. 3	1.20	13	9.8	108	0.12
No. 4	1.10	11	10.2	102	0.11

TABLE V												
EXPERIMENTAL LITHOGENESIS												
Functional Parameters the Week of Percutaneous Inoculation with Nanobacteria												
Rats	Ingested	Dilution	Vol./mi.	CrO	CrO	O Urea	CrS	O Ur. A	Ur./Cr	O Ur. A	O Prot.	CGr
	(ml H_2O)			(mg/24h)	(values expressed in mg/dl)					(expressed in mg/24h)		(µl/ml x 100 g)
No. 1	10.2	9	0.0062	10.2	114	59.6	1.5	12.8	0.11	1.1	3.15	329
No. 2	10	10	0.0069	9.6	96	52.5	1.4	12	0.12	1.2	3.30	337
No. 3	10.2	10	0.0069	9.9	99	47.4	1.3	13.4	0.12	1.3	4.20	375
No. 4	10	10	0.0069	8.2	82	44.6	0.9	9.5	0.11	0.9	2.50	433
Normal values in rats: CrS = 0.3-0.5 mg/dl. Glomeruler filtrate – 1100 µl/ml x 100 g *Proteinuria/24h = 2-3 mg*												

TABLE VI					
EXPERIMENTAL LITHOGENESIS					
Calcium and Phosphorous Values, Days (7) and 14 After Inoculation					
Rats	CaS	CaO	CaO	P O	P O
	(mg/dl)	(mg/24h)	(mg/dl)	(mg/24h)	(mg/dl)
No. 1	(8.7) 9.4	(2.3) 0.95	(25.5) 13.7	(13.5) 14.6	(149) 209
No. 2	(8.6) 9.2	(1.3) 0.8	(13) 12.6	(12) 9	(122) 146
No. 3	(8.8) 9.1	(0.9) 1.3	(9.4) 16	(9.3) 17	(93) 212
No. 4	(8.8) 9.4	(2) 0.6	(20) 9	(10.2) 5.7	(102) 80

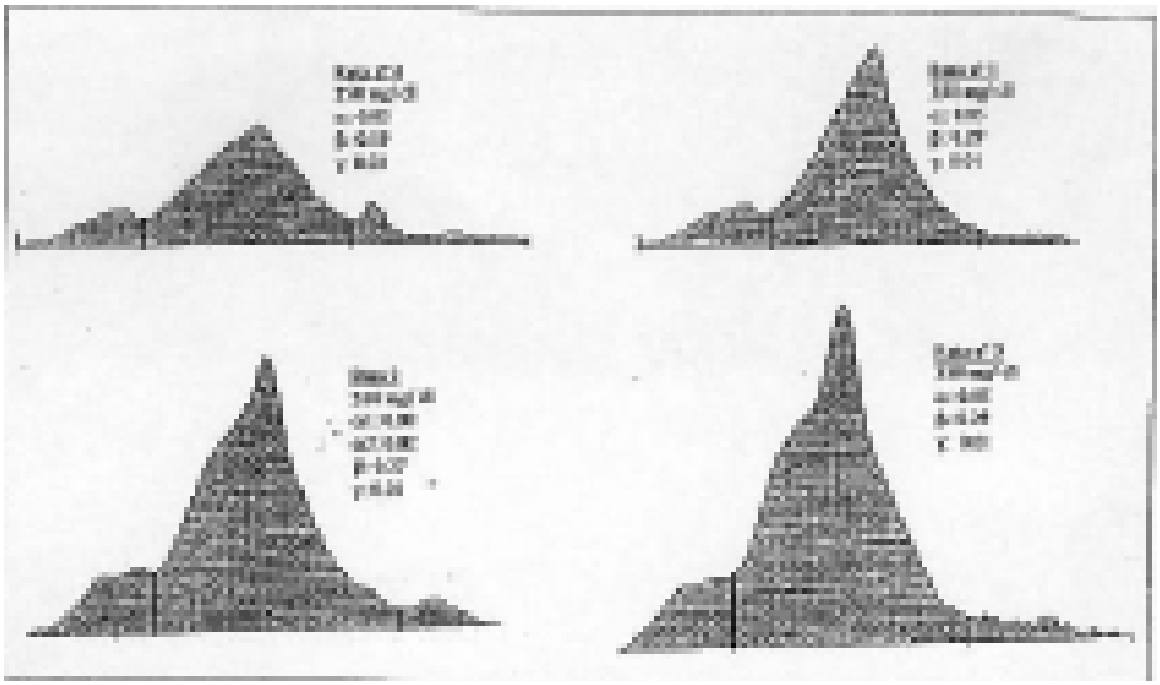

[Graph: Rata = rat]
Fig. 5: EPS urinary proteins of the inoculated rats on Day 7. Rat No. 4 is the control. The nanobacteria inoculations were progressive: Rat No. 1 = a, Rat No. 2 = 2a, Rat No. 3 = 5a, with a being the stock solution of nanobacteria.

On the twelfth day, an AP x-ray of the abdomen was taken of each rat. A second lateral x-ray and an abdominal ultrasound were performed on Rat No. 3.

Three weeks into the experiment, an x-ray of the abdomen and urographs were taken of Rat No. 2. When calcium deposits were seen in Rats Nos. 2 and 3,it was decided to euthanize them in order to confirm the existence of an obstructive lithiasic uropathy in the inoculated kidney.

RESULTS

I – Basal Data relative to water consumption, diuresis, serum and urinary creatinine, calcium and phosphorous appear in Tables II, III and IV.

II – Changes the first week.

II. A – Physical data:

The rats' tolerance was generally good, with the exception of three observations.

1 – Initial generalized weight loss: from 150 g to 140 g.

2 – Also in Rat No. 3, left nephromegaly of 24 mm compared to 19 mm measured in the contralateral kidney.

3 – Urine with turbidity of +++ /+++++ in Rat No. 3, and to a lesser degree ++/+++++ in Rats Nos. 1 and 2. In Rat No. 4, the turbidity level was +/+++++.

II B. Analytical Data:

1 – The pH, measured in fresh urine, was close to 8.

2 – Based on normal renal function parameters, on the seventh day, the control rat (No. 4) had a glomeruler filtrate of 30%; in Rats Nos. 1, 2 and 3, the filtrate was 24, 29 and 34% respectively, Tables II and V.

3 – On the seventh day, the urinary proteinogram showed an increase in b-globulin, a peak proportional to the bacterial load, Fig. 5.

4 – Calcemia levels, which dropped during the week of inoculation, recovered at 14 days, Table VI.

5 – A decrease was noted in the urinary calcium excretion figures for Rats Nos. 1, 2 and 3. This progressive decrease is interpreted as a *sequestration phenomenon*, which appears to be directly related to the degree of aggression. This is a finding that is accompanied, to a lesser

extent, by a decrease in the urinary excretion of phosphates, Table VI.

6 – No effects on uric acid parameters are seen.

7 – No glucosuria is observed in any of the test animals.

III – Medium-term results (12-14 days after inoculation):

1 – Blood and urinary creatinine values recovered 14 days after inoculation, Table VII.

2 – Image studies. Radiologically, Rats Nos. 1, 2 and 4, which was the control, showed a typical air pattern in the abdomen. No calcifications were detected in the renal areas or in the other intra-abdominal organs.

Rat No. 3 showed an air pattern that corresponded in the lateral plate to the content of the intestinal loops in front of the left kidney. Upon palpation, this kidney was larger in size than the contralateral kidney and than it was prior to being injected. It measured 24 mm in length in the abdominal ultrasound. The right kidney measured 19 mm.

IV – Results at 3 Weeks:

1 – In the rats that were subjected to higher nanobacteria loads, Rats Nos. 2 and 3, the abdominal x-ray revealed the presence of a calculus in the left kidney, and the urographs showed an obstructive uropathy on the pyelic level (Figs. 6 and 7). Radiologically, there were no calcifications in Rat No. 1 and Rat No. 4, which was the control rat.

DISCUSSION

Starting with the basal parameters for rats weighing approximately 150 g, we made a series of observations beginning in the first week of inoculation:

1 – General 10-g weight loss, which stabilized at approximately 140 g.

2 – Renal failure, measured by creatinine clearance, partially reversible at one week.

3 – Selective type b-microglobulin proteinuria revealing an acute process observed on the seventh day, which was negated one week later.

4 – The appreciable decline in calcemia and the *sequestration* of urinary Ca (23) shows its participation in the renal failure.

Fig. 6: Abdominal x-ray of Rat No. 2 at 21 days. A radiopaque image is noted on the left renal area.

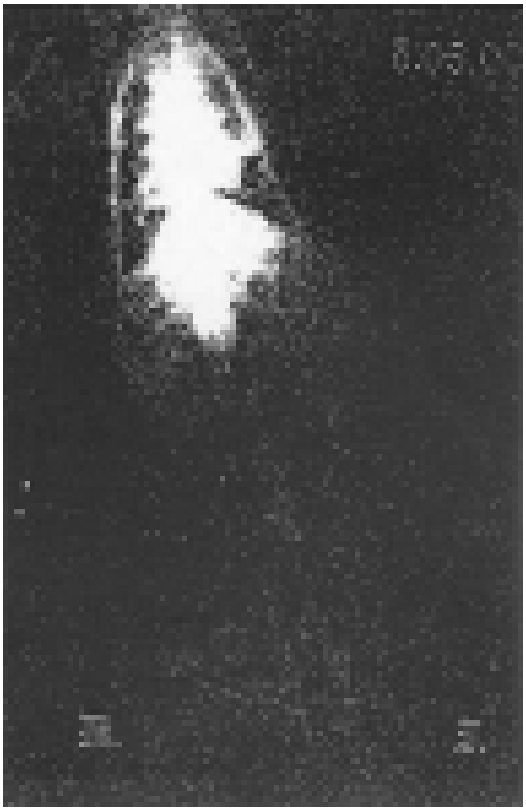

Fig. 7: Film of the urographs performed on Rat No. 2. Lithiasis is noted in the left kidney with a large obstructive pyelocaliceal uropathy and very little ureteral permeability.

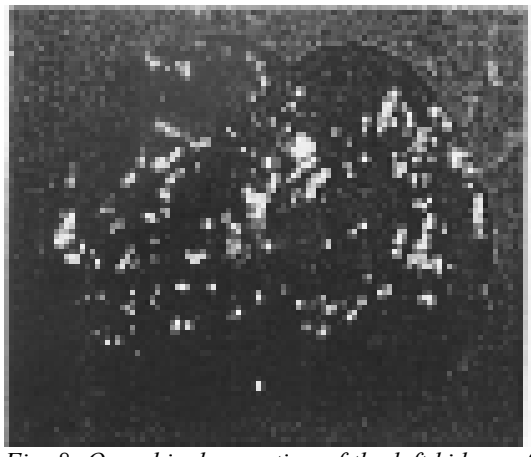

Fig. 8: Open bivalve portion of the left kidney of Rat No. 3. A pyelocaliceal lithiasic mass x 3 is noted.

The conversion of plasma calcium to [Ca++]i (intracellular), or *sequestration*, is a process that has a double effect on oxidative phosphorylation and the synthesis of ATP, Arnold (24). In our country, Ruiz Marcellán has been assessing renal damage on the enzymatic level produced by extracorporeal shock wave lithotripsy (ESWL) (25). Wetzels (26) identifies a sequence of processes that we can systemize as follows:

- Activation of Phospholipase A_2 (PLA2) that induces changes in the permeability of the plasma and mitochondrial membranes.

- Activation of the calcium-dependent cytosolic proteases, most importantly *calpain*.

- Direct or *calpain-induced* alteration of the structure and function. Effects of the activity of a powerful modulator of renal hemodynamics, nitric oxide (NO), by means of the calcium-dependent synthesized nitric oxide, Moncada (27).

- Activation of proteolytic processes of the *cytoskeleton*, or directly on the action of proteins of the same cytoskeleton (28).

- There appears to be an effect on *apoptosis* or programmed cellular death, either directly due to the increase in [Ca++] i or due to changes in the cytoskeleton, *calpain-induced* (29 and 30).

- The response could end up producing *heat shock proteins* (HSP 90, 70, 60, 27, *Ubiquitin*) (31 and 32) and the formation of Tamm-Horsfall intratubular glycoprotein cylinders (33, 34) such as PAS-positive cylinders that obstruct the collector tube (35, 36).

We still cannot determine in depth the mechanisms that triggered the lithogenesis. We have data at 21 days in the abdominal x-ray for Rat No. 3 (75 kv 100 mA/25 ms) of the formation of a radiopaque image on the renal area of the left side and in urographs performed on Rat No. 2 that clearly show the presence of an obstructive lithiasic uropathy as noted in the renal pelvis of the removed portion corresponding to the left kidney of Rat No. 3 (Fig. 8). The fact that no lithiasic images are noted at this time in Rats Nos. 1 and 4, the control rat, lead us to think that the surviving bacterial load not destroyed by the animal's defense mechanisms was responsible for the *in situ neolithogenesis*. The sufficient population of *nanobacteria* acted as a nucleation center commencing with the experimental puncture (as authentic *spherulites* assumed by Cifuentes, inducers of heterogeneous nucleation phenomena) as we find in the clinic (Figs. 9 and 10) when the calculi are not fragmented by extracorporeal lithotripsy (ECL) (37).

TABLE VII
EXPERIMENTAL LITHOGENESIS
Renal Function Data, Weeks 1 and 2 after Nanobacteria Inoculation

Rats	Ingestion	Diuresis	Vol./min.	CrO	CrO	CrS	CCr
	(ml H2O)	(ml)		(mg/24h)	(values in mg/dl)		(µl/min. x 100 g)
No. 1	(10.2) 12.5	(9) 7	(0.0062) 0.0048	(10.2) 10	(114) 143	(1.5) 0.53	(234) 648
No. 2	(10) 7.5	(10) 6.2	(0.0069) 0.0043	(9.6) 9.2	(96) 149	(1.4) 0.58	(240) 563
No. 3	(10.2) 15	(10) 8.1	(0.0069) 0.0050	(9.9) 11.6	(99) 144	(1.3) 0.55	(267) 750
No. 4	(10) 10	(10) 10	(0.0069) 0.0069	(8.3) 6.8	(82) 95	(0.9) 00.50	(308) 467

Abbreviations as in Table V. Note the recovery toward the Crs and CCr basal values from Table II.

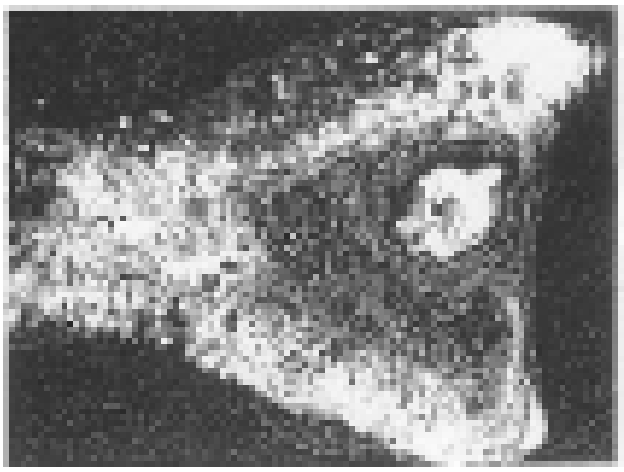

Figs. 9 and 10: Core of lithiasic formation. Around it, the calculus of another principal composition, but distinct from that of the initial core, has formed. (Urolithiasis Laboratory. Hospital Ramón y Cajal)

CONCLUSIONS

Translumbar percutaneous renal puncture (PRP) has permitted performing laparotomy without antibiotic coverage, which was the main difficulty of the experimental model of lithogenesis. Nanobacteria were cultured successfully, but not without difficulty, and formation of calculi in the rat pyelocaliceal system was achieved. This experimental model will provide further insight into lithogenesis and will allow us to find the answers to some of the many questions concerning this condition that remain.

ACKNOWLEDGEMENTS

The following people collaborated on this experimental project:

1 – Dr. Ari Tuuri, Finland.
2 – Dr. Pedro González Porqué. (Department of Immunology).
Ms. Elena Cardero, ATL.
3 – Miguel Sánchez Encinar, Juan Luis Sanz, Ana Linares Quevedo and Javier Sánez, Residents in the Department of Urology of the Hospital Ramón y Cajal in Madrid.
4 – Elena Navarro, Biologist (Department of Immunology).
5 – Drs. Servio Ávila Padilla, Juan Villar-Palasí, César Cabeza and Isabel Pignatelli (Department of Clinical Biochemistry).
Manuel Manero and Carmen Santiuste, Residents.
Francisco Delgado and Ángel Terrón, ATL.
6 – Clara Redondo (Department of Pathological Anatomy, Electronic Microscopy).
Ms. Valvanera, ATL.

Thanks to everyone for making this possible.